25th ABCM International Congress of Mechanical Engineering
October 20-25, 2019, Uberlândia, MG, Brazil

COBEM-2019-0692
FINITE VOLUME METHOD APPLIED TO A NEW GEOMETRY FOR SUBSEA FREQUENCY INVERTER ENCLOSURES

Lucas Andrade Militão
Diego dos Santos
Polo – Research Laboratory for Emerging Technologies in Cooling and Thermophysics
Federal University of Santa Catarina, Florianópolis, SC, 88040900, Brazil
lucas.militao@polo.ufsc.br
diego.santos@polo.ufsc.br
Douglas Mateus Machado
Polo – Research Laboratory for Emerging Technologies in Cooling and Thermophysics
Federal University of Santa Catarina, Florianópolis, SC, 88040900, Brazil
douglas.machado@polo.ufsc.br
Alexandre Kupka da Silva
LEPTEN – Energy Conversion Process Engineering and Technology Laboratory
Federal University of Santa Catarina, Florianópolis, SC, 88040900, Brazil
a.kupka@ufsc.br
Jader R. Barbosa Jr.
Polo – Research Laboratory for Emerging Technologies in Cooling and Thermophysics
Federal University of Santa Catarina, Florianópolis, SC, 88040900, Brazil
jrb@polo.ufsc.br

Abstract. *Frequency inverters are being used in a new type of depth sea installation: subsea electrical grids. One major challenge in such location is to maintain the temperature of electronic components below specified limits. The thermal management of such devices is performed throughout the use of different types of thermal models, according to the literature: analytical, numerical or thermal network model. The present work proposes the use of a finite volume method, with the support of a thermal network model (representing the entire cooling system of the subsea frequency inverter), to accurately predict the temperature distribution in the vicinity of the electronic components of the inverter circuit. An experimental apparatus was designed and built using a genetic algorithm to determine the dimensions of the system for maximum performance. External water temperatures from 10 to 25 ºC were considered, and total power dissipated from 200 to 600 W. The experimental results presented temperatures in the vicinity of the electronic components below the theoretical limits, for all test points. A maximum deviation of 7,2 ºC was obtained when comparing the numerical with the experimental data, for the measuring points close to the electronic components.*

Keywords: *Finite Volume Method, Natural Convection, Subsea Frequency Inverter Enclosure*

1. INTRODUCTION

The oil industry, motivated by the necessity of finding new oil extraction points, has been exploring deeper ocean waters. A requirement to extract oil at such depth is the establishment of subsea electrical grids, that rely strongly on frequency inverters to promote an efficient and trustworthy operation. There are some major obstacles in using this equipment at such location: ambient pressure of approximately 300 bar (for depths of 3000 m) and maintaining the temperature of electronic devices below specified values for safe operation, generally 80-90 ºC in the vicinity of the circuit components (Franchi, 2009).In order to provide the necessary thermal management of such power electronic devices, a large variety of thermal models have been developed in the last decade. Qian et al. (2017) made a review of available studies regarding thermal models to predict the temperature of power electronic devices such as IGBTs (Insulated Gate Bipolar Transistors), and found that they can be divided into analytical, numerical and thermal network models. Reichl et al. (2015) used a 3D finite-difference model, with input thermal data obtained from an electrical simulator of the electronic components, to predict temperatures at a multilayered and multicomponent power circuit, considering transient state. Model data was validated throughout the comparison with experimental data from a test circuit. A fixed temperature distribution was assumed at the lower surface of the board, with the sides and non-dissipating areas at the top considered to be adiabatic. Good agreement was obtained between numeric and experimental results.

The present work proposes the use of a numerical model, developed using the finite volume method, to determine within an acceptable accuracy, the temperature distribution in a given power electronic circuit, located at a subsea

enclosure with innovative geometry, filled with isolating oil. The boundary conditions such as heat transfer coefficient and external reference temperature are provided by a thermal network model representing the entire cooling system of the subsea frequency inverter, and developed by Militão *et al.* (2019). The heat transfer coefficient is corrected according to the vertical coordinate of the finite volume elements in order to provide better accuracy, throughout a correction equation obtained by a scale analysis of the relevant parameters.

2. MODELING

2.1 Proposed geometry and thermal network model

The suggested geometry consists of three curved circuit boards, centered radially and vertically, inside a circular annulus enclosure, of internal radius *r*, and external radius *R*, and height L_o.

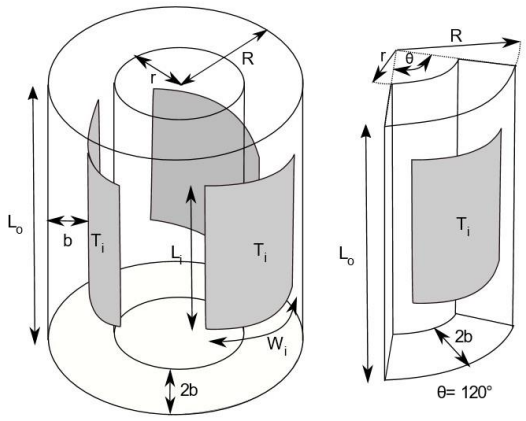

Figure 1. Circular annulus geometry proposed for the frequency inverter enclosure and geometry cell considered for mathematical modeling.

The objective of such geometry was to enhance heat transfer and to provide a more compact system, by distributing the circuit components in such manner that the fluid volume to surface area ratio is advantageous. Besides, the presence of an internal region for the water to ascend gives the chance of the formation of a vertical channel heat transfer condition, that is beneficial from heat transfer viewpoint.

The thermal network model comprises all existing thermal resistances and component temperatures in the proposed passive cooling system, in order to make it feasible to estimate circuit board temperatures, once boundary conditions are known. Estimating the external thermal resistances, associated with natural convection, and the ones representing heat conduction is an easy task, since there are available heat transfer correlations for such cases in the literature. But, defining the thermal resistances associated with the heat transfer between the circuit boards and the internal enclosure walls is rather difficult, because there is no existing correlation for such phenomena when the geometry presented on Fig.1 is considered. The solution encountered by the authors to this issue was to adapt an existing correlation, proposed by (Teertstra et al,2004), for the heat transfer between a convex isothermal body inside an arbitrarily shaped concave isothermal enclosure. In order to make the mathematical modeling feasible from a technical viewpoint, only a third of the geometry was considered, relying on physical and heat transfer symmetry. The lateral surfaces of this geometry are adiabatic, since there is no significative heat transfer between adjacent convective cells.

The thermal compact model considers steady regime operation for the whole system, therefore, a constant dissipation power,Q is considered at the circuit board, with a fixed external ambient water temperature on the exterior of the enclosure, defined as T_{amb}. A representation of the thermal network is presented on Figure 2.

The area used for the calculation of the thermal resistances on the enclosure internal walls is based on a weighted area calculation:

$$\widetilde{A_n} = \frac{A_n}{A_o}.A_i \tag{1}$$

where the subscript n refers to the surface analyzed, A_o is the total enclosure internal area and A_i is the wetted area of the inner body.

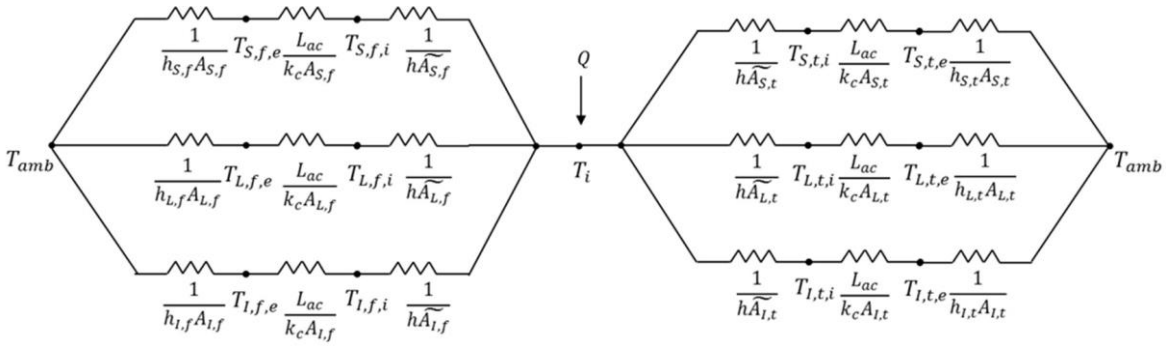

Figure 2. Thermal network for the subsea passive cooling system.

The temperature T_o(refered as T_{ref} in the finite volume model) is the enclosure internal walls averaged temperature, calculated by the following equation:

$$T_o = \frac{\sum_{j=1}^{k} T_j A_j}{\sum_{j=1}^{k} A_j} \tag{2}$$

where A_j is the surface area of the internal wall j, and T_j is the surface temperature on this same internal wall.

The heat transfer correlations used to define the heat transfer coefficients, as well as the iterative Gauss-Seidel Solver procedure to determine the temperature at the nodes can be seen at Militão *et al. (*2019).

2.2 Finite volume model

The problem to be addressed by the finite volume code consists in an aluminum rectangular plate, with external natural convection with at a known external temperature, T_{ref}(equal to T_o calculated by the thermal compact model) and a heat transfer coefficient h, and with prescribed heat flux ,q",at five spots in its surface(where the heat dissipating resistors are located). Both the reference temperature and the heat transfer coefficient are obtained from the thermal network model. The figure below illustrates it:

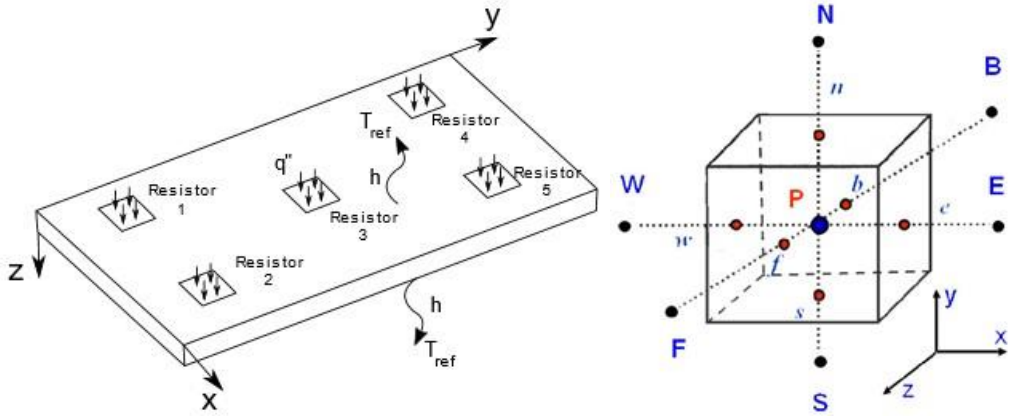

Figure 3. Aluminum rectangular heat plate with prescribed heat flux and convective flux on the external surfaces (Left) and tridimensional elementary volume considered to obtain the approximate equations (Right).

It can be noted that the analyzed domain does not represent the protruding fins of the heat sink. They are not modelled because the influence of the fin assembly at the surface of the heat sink is already accounted for in the heat transfer correlation used to determine the enclosure internal heat transfer coefficient, more specifically being represented by the body gravity function term, $G_{\sqrt{A_i}}$. Besides, since the Biot number, $Bi = \frac{hL}{k}$, is very small (due to the high conductivity of aluminum and small thickness of the base plate), the temperature distribution will not be significantly affected by the exclusion of the fins, once the thermal resistance is mainly convective.

The starting point for the development of the model is the tridimensional heat diffusion differential equation for transient regime, in its conservative form, as presented below:

$$\frac{\partial}{\partial t}(\rho T)=\frac{\partial}{\partial x}\left(\frac{k}{c_p}\frac{\partial T}{\partial x}\right)+\frac{\partial}{\partial y}\left(\frac{k}{c_p}\frac{\partial T}{\partial y}\right)+\frac{\partial}{\partial z}\left(\frac{k}{c_p}\frac{\partial T}{\partial z}\right)+S \tag{3}$$

where k is the thermal conductivity (W/m.K), ρ is the density of the material, in kg/m^3, c_p for the specific heat (J/kg.K) and S for the source term. Since only the steady regime solution matters to the heat transfer problem we analyze in this study, the transient term can be disregarded. Another term that can be discarded is the source term, since there is not internal heat generation. By simplifying the above equation through the elimination of these terms and considering the material as isotropic, we get to:

$$0=\frac{k}{c_p}\left[\frac{\partial^2 T}{\partial x^2}+\frac{\partial^2 T}{\partial y^2}+\frac{\partial^2 T}{\partial z^2}\right] \tag{4}$$

Considering an elementary volume at the interior of the domain, without prescribed heat flux and external convection, and integrating the Eq. (4) in three dimensions, we get to:

$$\frac{k}{c_p}\left[\left(\left.\frac{\partial T}{\partial x}\right|_e-\left.\frac{\partial T}{\partial x}\right|_w\right)\Delta y\Delta z+\left(\left.\frac{\partial T}{\partial y}\right|_n-\left.\frac{\partial T}{\partial y}\right|_s\right)\Delta x\Delta z+\left(\left.\frac{\partial T}{\partial z}\right|_f-\left.\frac{\partial T}{\partial z}\right|_b\right)\Delta x\Delta y\right]=0 \tag{5}$$

Dividing the above equation by the elementary volume $\Delta x\Delta y\Delta z$, and approximating the derivatives at the interfaces by a central differencing scheme, and arranging all terms, we finally get to:

$$(2A_x+2A_y+2A_z)T_P-A_x(T_W+T_E)-A_y(T_N+T_S)-A_Z(T_F+T_B)=0 \tag{6}$$

where $A_x=\frac{k}{(\Delta x)^2}$, $A_y=\frac{k}{(\Delta y)^2}$ and $A_z=\frac{k}{(\Delta z)^2}$. The boundary conditions, such as the prescribed heat flux and convective heat transfer, were introduced appropriately at the approximate equations for the volumes where they belong through an energy balance at the volume interface. For instance, for a generic interface I where exists external convection or prescribed heat flux in a normal direction l pointing outwards, the heat that is extracted or enter the volume by diffusion must be equal the heat removed or given through the interface, q''_f (W/m²):

$$-k\left.\frac{\partial T}{\partial l}\right|_I=q''_f \therefore \left.\frac{\partial T}{\partial l}\right|_I=-\frac{q''_f}{k} \tag{7}$$

The term q''_f was calculated by using the energy balance at boundary volumes method (Maliska,1995). For the convective boundary condition, and a distance from the center of the volume to the boundary of $\Delta l/2$, we have:

$$q''_f=\frac{-h}{\left(1+\frac{h\Delta l}{2k}\right)}(T_{ref}-T_P) \tag{8}$$

When the mixed boundary condition of prescribed heat flux and convective heat transfer is considered, the equation becomes:

$$q''_f=\frac{-h}{\left(1+\frac{h\Delta l}{2k}\right)}(T_{ref}-T_P)+q'' \tag{9}$$

The heat flux input q'' is provided by the user based on the power dissipation for each electronic component in the domain.

In order to mimic the heat transfer coefficient variation along the vertical coordinate (y) of the circuit board, a correction equation is used, obtained by a scale analysis of the known relation between the Nusselt number and Rayleigh number for natural convection at the laminar regime ($Nu_y \sim Ra_y^{1/4}$):

$$h(y)=h_{L/2}\left(\frac{\Delta T}{\Delta T_{L/2}}\right)^{1/4}\left(\frac{L}{2y}\right)^{1/4} \tag{10}$$

where $h_{L/2}$ is the mid-half heat transfer coefficient, provided by the thermal network model, $\Delta T=\left(T_{ref}-T_P\right)$ and L is the vertical length of the domain. As mentioned by Incropera *et al*. (2011), the procedure for calculating the heat transfer coefficient in such manner is iterative, given its dependence with temperature. Therefore, it must be calculated during a determined number of iterations, until convergence for the heat transfer coefficient and the temperatures is attained.

A residue parameter $\gamma(y)$ was defined, based on the heat transfer coefficient value for each surface volume location:

$$\gamma(y)=h(y)_i-h(y)_{i-1} \tag{11}$$

For convergence to be obtained, the condition $\gamma(y) < 0{,}01$ had to be satisfied for all surface volumes where convection occurs.

The solution of the finite volume code was done by using a direct sparse matrix solver, that considers only the non-zeros values of the coefficient matrix to obtain the solution, making it faster and allowing that more refined grids are used, by using the same computational resource. The implementation of the finite volume method was done using Python 2.7 language.

3. EXPERIMENTAL APPARATUS

An experimental apparatus was built in order to validate the numerical model. A three-phase multilevel NPC frequency inverter circuit, dissipating 420 W of maximum power was chosen as a model to build the experimental prototype. An external temperature of the water of 25 ºC was considered, based on literature data for subsea inverters operating at seawater temperature. The dimensions of such device were determined by using a genetic algorithm, that provided the optimal dimensions of the geometrical parameters, for maximum performance.

A genetic algorithm was built to create a population of distinct individuals (cooling systems with distinct geometric parameters in an established range of values for each variable). Through the use of pairing, reproduction, mutation and natural selection mechanisms, the algorithm obtained the system that provides the best performance by using an objective function (for the actual study, the thermal network model).

The individual's genes, were represented by the geometric parameters : the external radius, the height, the aspect ratio(defined by the ratio of the enclosure height,L_o ,and the gap between the circuit board and enclosure wall,b) .In order to determine the optimal values of such parameters(hence the optimal cooling system)the objective function was used, considering the cost as the total volume of dielectric fluid inside the enclosure, having the maximum circuit board temperature of 75 ºC as a restriction. The optimal values obtained for the stablished parameters were: $R = 0{,}20\ m$, $r = 0{,}07\ m$, $L_o = 0{,}40\ m$ and $Ar = \frac{b}{L_o} = 6{,}66$.

The enclosure was built in acrylic to facilitate water leakage detection, from the exterior of the prototype to the inside of it. In order to represent the inverter circuit, a circuit containing thirty 220 **Ω** resistors was built. Each phase of this circuit consisted of two circuit boards with five resistors each, distributed evenly on the circuit board. The choice of the resistors model was realized taking in consideration the necessary characteristics to the project, as maximum capacity of dissipation relevant to the nominal values and its geometry, that is very similar to the geometry of the transistors used in frequency inverters. Standard commercial aluminum heat sinks were attached to the resistors, just like in the assembly of real inverter circuits. Each pair of heat sink-circuit board, representing one phase of the electrical circuit, was assembled forming an 150º angle between them, in order to represent in the best possible way, the curved surfaces considered at the thermal network model. Finally, each heat sink-circuit board pair was attached to the enclosure. The following image shows the enclosure, the heat sink-circuit board pair and the final assembled system:

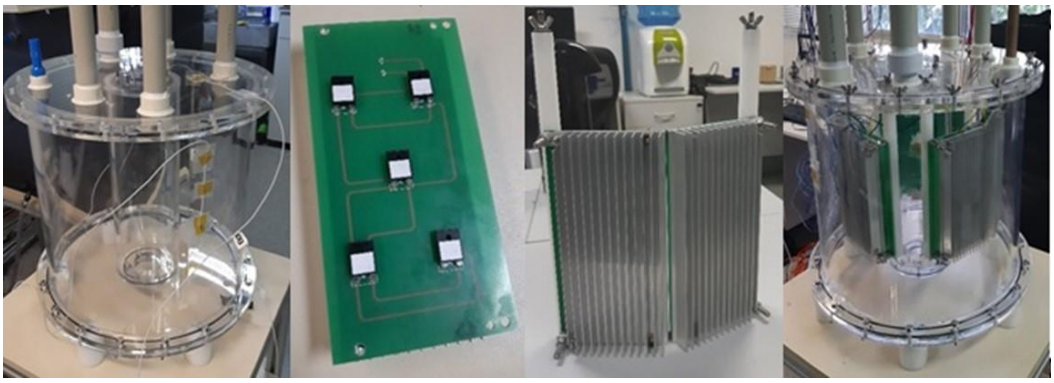

Figure 4. From left to right: Acrylic enclosure, circuit board with the resistors, assembled heat sink-circuit board pair, assembled system.

The experimental apparatus has to be able to emulate in the best way the environment which the subsea frequency inverters operate, in order to properly evaluate heat transfer and measure steady regime temperatures of the prototype components. That means that the exterior of the enclosure must be cooled by a natural convection water stream on its outside surfaces. To properly do so, a water circuit was built, composed by a thermostatic bath circulator, a glass water tank and a water flowmeter. The prototype was positioned inside the water tank, and filled with MIDEL® 7131 fluid, an electric isolating oil already used in patented subsea frequency inverter enclosures, such as Aarskog (2013) device. The inlet and outlet ports of the water tank were positioned in such a way that the natural convection flow is not disturbed by the extraction and insertion of water. The role of the thermostatic bath was to cooldown the heated-up water that ascended vertically from the exterior of the submerged prototype.

The resistors at two heat sink pairs were instrumented using RTDs and thermocouples, with the first used to instrument the resistors localized in the geometric center of heat sink surface and the latter to instrument the remaining resistors. For the points located in the walls of the enclosure, internal and external, the RTDs were used, in order to provide better accuracy in these points and due to easier fixation, that they have compared to thermocouples when flat surfaces are regarded. For the fluid temperature measuring points, thermocouples were considered. All measuring points are represented in the image below, with the fluid measuring points displayed in black dots and the wall and heat sink measuring points represented by gray dots.

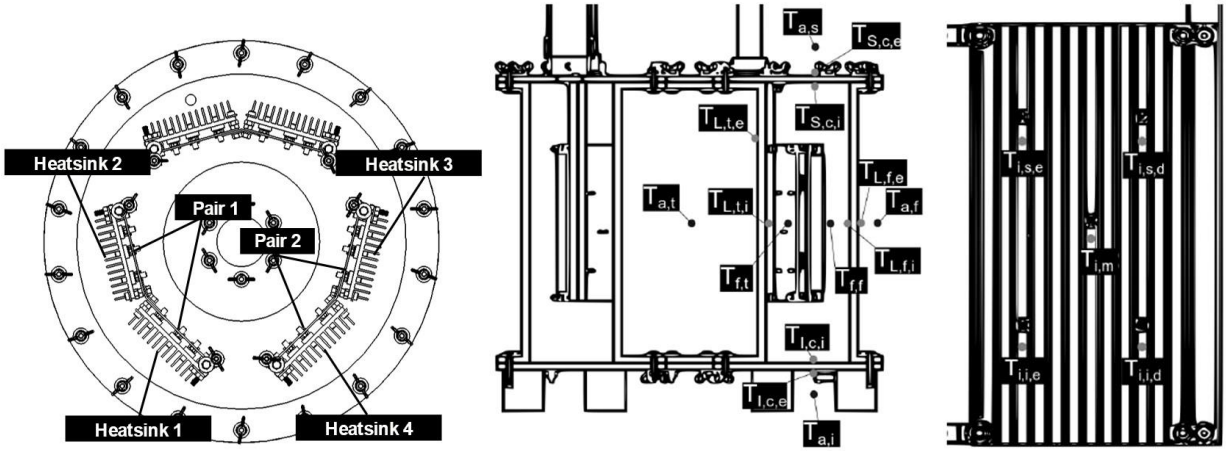

Figure 5. From left to right: Superior view of the enclosure with components identification, Lateral section view of the prototype with the measurement points displayed and frontal view of one heat sink with appropriate measuring points.

All the circuit boards were supplied with regulated voltage, and data was acquired using a National Instruments series SCXI-1000 acquisition system. The process started through the power up of the acquisition system and posteriorly of the experimental apparatus. The voltage regulator was adjusted for the voltage that provides the power dissipation necessary at the resistors and the thermostatic bath was adjusted to the desired external water temperature. A waiting time of 2 to 3 hours for the system to achieve steady regime was observed, and after that the data was recorded during 3 minutes in an acquisition frequency of 60 Hz. Afterwards, new values of power and temperature were adjusted and the described procedure was repeated for the next experimental test. The tests were performed for the following external water temperatures: 10, 15, 20 and 25 ºC, with the following power dissipation values for each circuit board pair :66, 100, 140, 166 and 200 W. In order to increase data reliability, repeatability tests were performed for all external water temperatures with the power dissipation values of 66, 140 and 200 W.

4. RESULTS AND DISCUSSION

Experimental data was obtained with an expanded uncertainty of 0,1 ºC for the measured temperatures and a maximum expanded uncertainty of 2,3% for the Nusselt number and 2,8% for the Rayleigh number. Each temperature measurement presented for the heat sink is an arithmetic mean of the corresponding points on the circuit board pair. Numerical results were obtained by using a finite volume grid with 17940 elements, each one with dimensions 2x2x1,67 mm, and with an extremely low energy balance residue, with the highest residue being $-1{,}25x10^{-4}$ %, what is expected, since the finite volume method requires that energy is conserved. The mesh size was defined based on a mesh convergence study, considering meshes with elements sizes of 1x1x1,67 mm,2x2x1,67 mm and 4x4x1,67 mm. No significative difference was observed between the more refined mesh and the mesh utilized in this study.

The measured values for the temperatures at the internal and external enclosure walls, for the reference condition of 25 ºC of external water temperature, are presented on Figure 6. For the same dissipated power on the heatsink pair, a clear increase in the temperature values for internal and external walls is observed, when the distance from the measuring point

from the bottom of the enclosure is increased. This trend indicates the direction of the flow outside the enclosure, since the saturation of the boundary layer temperature as the water ascends in the exterior, depicts its capacity to extract heat, what certainly elevates the temperatures on the enclosure external surfaces, and consequently on the internal. Such behavior is a strong evidence on the ability of the experimental apparatus to promote natural convection on the exterior of the prototype, just like it happens in a real subsea inverter operation.

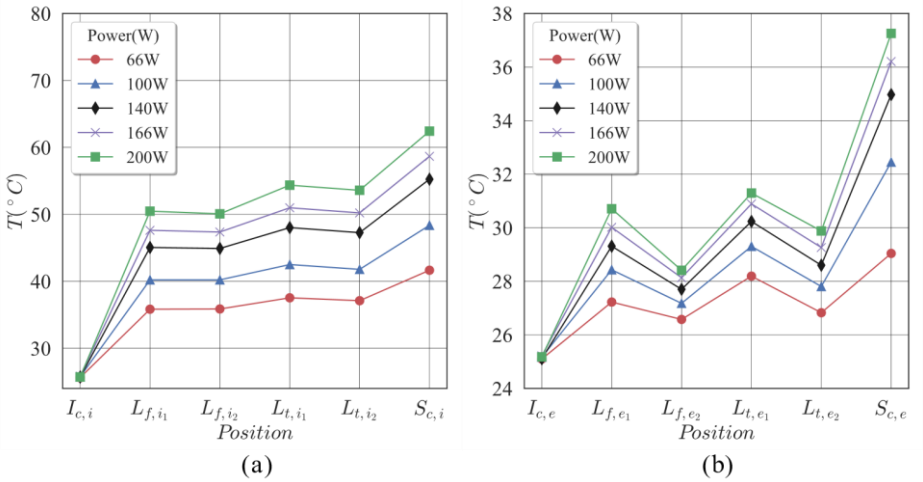

Figure 6. (a) Experimental temperatures on the internal enclosure walls. (b) Experimental temperatures on the external enclosure walls.

For the other external water temperatures used during the experimental tests, a similar behavior was observed, with a change in absolute values only due to changes in the temperature setpoint on the thermostatic bath.

The experimental values for the temperatures close to the resistors on both heatsink pairs are presented on Table 1, for the external water temperature of 25 ºC. It can be noted that even for the highest dissipated power on the resistors, the temperatures were in its majority below the limits specified in the literature for the vicinity of electronic components (Franchi,2009). The resistors that are positioned upwards on the heatsink presented higher temperatures than the ones located on the lower regions. That was expected, since as the fluid ascends the exterior of the heatsink, the boundary layer thickness decreases as heat is extracted from the heatsink, and so does the heat transfer capability of the dielectric fluid on that region. An increase on the temperatures as the power dissipation increases is also observed, what was expected, since more heat is being produced by the resistors for the almost same thermal resistance to the external environment.

Table 1- Experimental temperatures close to the resistors for an external water temperature of 25 ºC.

Region	**Position**	**Dissipated Power(W)**				
		66	**100**	**140**	**166**	**200**
Pair 1	T_{iie}	46,1	53,8	62,0	66,7	71,9
	T_{iid}	45,8	53,4	61,4	65,9	71,0
	T_{im}	47,7	56,3	65,4	70,7	76,6
	T_{ise}	48,3	56,6	65,5	70,5	76,2
	T_{isd}	48,5	56,8	65,6	70,6	76,2
Pair 2	T_{iie}	45,6	53,1	61,2	65,7	70,8
	T_{iid}	46,5	54,4	62,8	67,7	73,1
	T_{im}	48,0	56,5	65,6	70,9	76,9
	T_{ise}	49,6	58,6	68,2	73,7	80,1
	T_{isd}	48,0	56,2	64,9	69,8	75,3

The numerical temperatures obtained for the measuring points close to the resistors, when the reference condition of 25 ºC external water temperature is considered, are presented on Figure 7, accompanied by the absolute difference between the numeric values and the experimental ones, for both heatsink pairs. A small deviation is observed for lower dissipated power on the heatsink pairs and a higher deviation is observed for higher dissipation rates. A maximum deviation of 7,2 ºC is observed when comparing the data for the second heat sink pair, for the measuring point designated as $T_{i,i,e}$, and 200 W of dissipated power ,for 25 ºC external water temperature. A possible source of deviation is that the finite volume model uses as the reference temperature T_o, an average temperature of the internal enclosure walls, that presented a significant deviation from the average internal enclosure walls temperature calculated experimentally. The

data for the other external water temperatures presented smaller deviations, and in general, deviations lower than 5 ºC, what is an indicative that the model is able to predict temperatures in the vicinity of the resistors with some accuracy, but also shows that there is space for improvements.

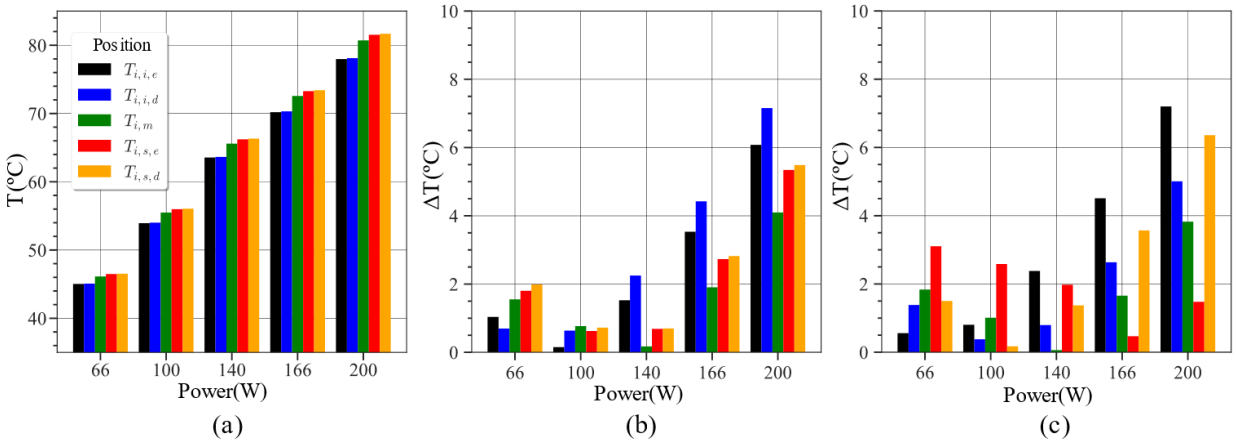

Figure 7. Comparison between numerical and experimental temperatures for the vicinity of the resistors and 25ºC external water temperature (a) Numerical data (b)Absolute difference for the first heatsink pair. (c)Absolute difference for the second heatsink pair.

The figures below present a temperature distribution at the surface of the heatsink in which the resistors are attached (upper surface), for all dissipated power values, when all external water temperatures are considered. An interesting effect that can be observed from the set of numeric data is the ability of the code to mimic the temperature increase as the vertical point coordinate raises.

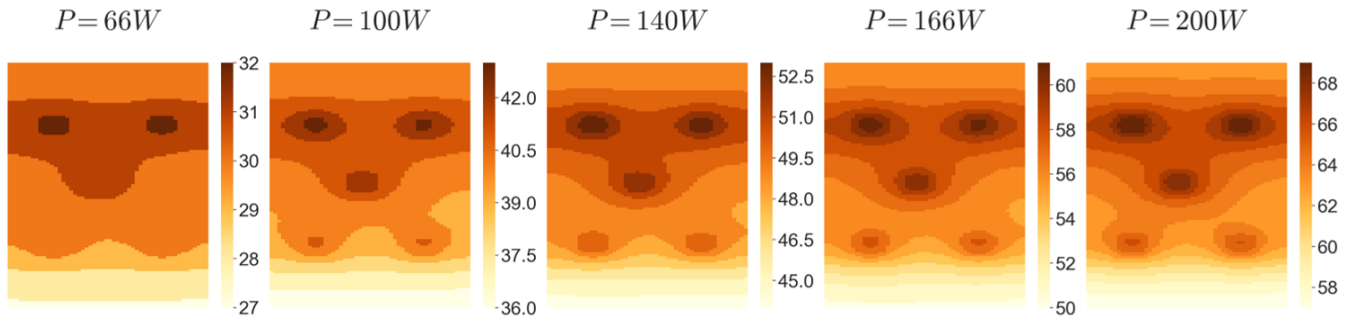

Figure 8. Temperature distribution on upper surface of the heatsink, for the whole range of dissipated power and 10ºC external water temperatures.

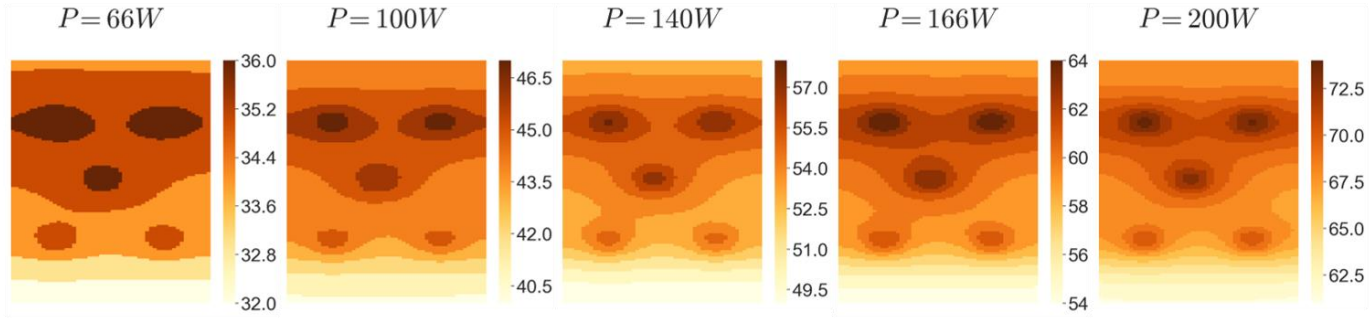

Figure 9. Temperature distribution on upper surface of the heatsink, for the whole range of dissipated power and 15ºC external water temperatures.

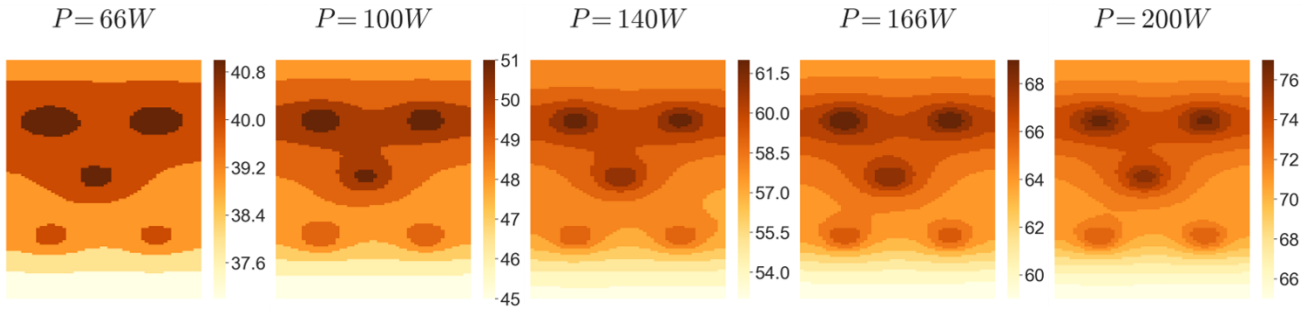

Figure 10. Temperature distribution on upper surface of the heatsink, for the whole range of dissipated power and 20ºC external water temperatures.

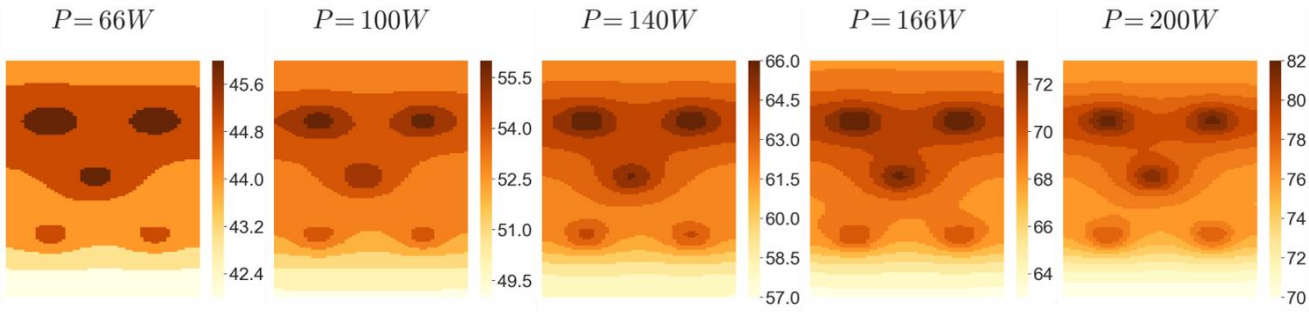

Figure 11. Temperature distribution on upper surface of the heatsink, for the whole range of dissipated power and 25ºC external water temperatures.

The highest temperature according to the temperature distribution plots occur, as expected, where the upper resistors are located, due to the decrease in the thermal boundary layer thickness, and consequently in the overall heat transfer rate across the heatsink surface. An interesting heat spreading effect is also observed, when isothermal regions are considered. This effect is more pronounced horizontally, since in this direction there is no change in the external heat transfer coefficient at the heatsink surface.

5. CONCLUSION

This study intends to predict within an acceptable accuracy, the temperatures of the electronic components of a subsea frequency inverter, throughout the use of a finite volume code, integrated with a thermal network mathematical model ,representative of the passive cooling system considered, that allows to estimate the key parameters for defining natural convection at the exterior of the circuit boards. First, a genetic algorithm is used, altogether with the thermal network model, to obtain the optimal dimensions of an acrylic prototype of the enclosure with the proposed geometry, for the reference conditions of 25 ºC external water temperature and 420 W of dissipated power, 140 W per phase. Once such dimensions were known, an experimental apparatus was built, to proper simulate heat transfer conditions of a real subsea inverter frequency operation.

Experimental data, for all external water temperature and dissipation rates, have shown temperatures, for the vicinity of all electronic components, below the specified limits on the literature. Therefore, the capability of the thermal network model to design a feasible subsea frequency inverter passive cooling system is proven. Besides, the new proposed geometry proved to be promising and to be worth of comparing with already existing subsea frequency inverter geometries, in order to assess its performance.

The numerical data presented temperatures, in general, with an average absolute deviation of 5 ºC, when all external water and dissipation rates are considered. A maximum deviation of 7,2 ºC was found for the second heatsink pair, when comparing numerical and experimental data, for 25 ºC external water temperature and 200 W of dissipated power. The accuracy obtained is acceptable, but it yet must be improved. The authors suggest developing a more refined thermal network model, or a more complete finite volume code, that also comprises the whole passive cooling system, and not only the heatsink pairs. This would lead to more precise reference temperatures and heat transfer coefficients, leading to more realistic boundary conditions, implying in more accurate electronic component's temperatures.

6. ACKNOWLEDGEMENTS

I would like to thank Rafael Valdir de Lima for assisting in the construction and design of the experimental apparatus of the present work, and the professor Carlos Renato Rambo that diligently supplied all necessary resources to this project throughout its coordination. I am also very grateful to Petrobras, that through Project 013/16, provided financial support and made this study feasible.

7. REFERENCES

Aarskog, F. G., 23 dez.2013. “Subsea converter device.” EUROPEAN PATENT APPLICATION.EP2958411A1,10pp.

Churchill, S.W.; Usagi, R., 1972. “A General Expression for the Correlation of Rates of Transfer and Other Phenomena”. AIChe Journal, Vol.16, No.6, pp.1121-1128.

Churchill, S.W.; Chu, H.H.S. ,1975. “Correlating Equations for Laminar and Turbulent Free Convection from a Horizontal Cylinder”. International Journal of Heat and Mass Transfer, Vol.18, pp.1049-1053.

Culham, R. J.; Yovanovich, M.M.; Lee, S,1995. “Thermal Modeling of Isothermal Cuboids and Rectangular Heat Sinks Cooled by Natural Convection.” In: IEEE TRANSACTIONS ON COMPONENTS, PACKAGING, AND MANUFACTURING TECHNOLOGY-PART A, Vol. 18, No.3, pp.559-566.

Franchi, C.M.,2009. *Inversores de frequência: teoria e aplicações*. Érica,São Paulo, 2 ed.

Johnson, R.W. ,2016. *Handbook of Fluid Dynamics*. 2 ed. Boca Raton : CRC Press.

Incropera, F. P.; Dewitt, D. P.; Bergman, T. L.; Lavine, A. S. ,2011. *Fundamentos de Transferência de Calor e Massa*. 6.ed. Rio de Janeiro: LTC.

Maliska, C. R.,1995. *Transferência de Calor e Mecânica dos Fluidos Computacional.* LTC,Rio de Janeiro.

Militão, L.A.; Barbosa Júnior, J.R.; Da Silva, A.K.; Dos Santos, D.M.; Machado, D.M., 2019. “ An innovative concept of a subsea frequency inverter cooling system”. Thermal Applied Engineering. *No prelo*.

Moran, W.R.; Lloyd, J. R., , 1974. “Natural convection Adjacent to Horizontal Surface of Various Planforms.” Journal of Heat Transfer, pp.443-447.

Qian, C.; Gheitaghy, A.M.; Fan, J.; Tang, H.; Sun, B.; Ye, H.; Zhang, G,2017. “Thermal Management on IGBT Power Electronic Devices and Modules”. *IEEE Access*, Vol.6, pp.12868-12884.

Reichl, J.; Ortiz-Rodríguez, J. M.; Hefner, A.; Lai, J.,2015. “3-D Thermal Component Model for Electrothermal Analysis of Multichip Power Modules with Experimental Validation.” In *IEEE TRANSACTIONS ON POWER ELECTRONICS*, Vol.30, No.6, pp. 3300-3308.

Teertstra, P.M.; Yovanovich, M.M.; Culham, J.R.,2004.“Models and Experiments for Laminar Natural Convection from Heated Bodies in Enclosures”.In: *2004 ASME Heat Transfer/Fluids Engineering Summer Conference*,Proceedings of HT-FED04, Charlotte,United States of America.

Teertstra, P. M.; Yovanovich, M.M.; Culham, J. R. ,2006. “Modeling of Natural Convection in Electronic Enclosures.” Journal of Electronic Packaging, Vol. 128, pp.157-165.

Yovanovich, M.M; Teertstra, P. ,2002. “Natural Convection Inside Vertical Isothermal Ducts of Constant Arbitrary Cross Section.” Journal of Thermophysics and Heat Transfer, Vol.16, No.1, pp.116-121.

8. RESPONSIBILITY NOTICE

The authors are the only responsible for the printed material included in this paper.